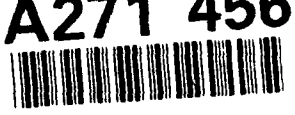

1. AGENCY USE ONLY (Leave blank)	2. REPORT DATE	3. REPORT TYPE AND DATES COVERED
	September 23,1993	Reprint

4. TITLE AND SUBTITLE
The Response of the Large Scale Ionospheric Convection Pattern to Changes in the IMF and Substorms: Results from the SUNDIAL 1987 Campaign

5. FUNDING NUMBERS
PE 61102F
PR 2311
TA G5
WU 02

6. AUTHOR(S)
M. Lester, O. de la Beaujardiere, J.C. Foster, M.P. Freeman, H. Luhr, J.M. Ruohoniemi, W. Swider*

7. PERFORMING ORGANIZATION NAME(S) AND ADDRESS(ES)
Phillips Lab/GPS
29 Randolph Road
Hanscom AFB, MA 01731-3010

8. PERFORMING ORGANIZATION REPORT NUMBER
PL-TR-93-2207

9. SPONSORING/MONITORING AGENCY NAME(S) AND ADDRESS(ES)

10. SPONSORING/MONITORING AGENCY REPORT NUMBER

11. SUPPLEMENTARY NOTES
*AUTHOR AFFILIATIONS ON NEXT PAGE
Reprinted from Ann. Geophysicae 11, 556-571 (1993)

12a. DISTRIBUTION/AVAILABILITY STATEMENT
Approved for public release; Distribution unlimited

12b. DISTRIBUTION CODE

13. ABSTRACT

Abstract. This paper reports multi-point observations of ionospheric convection made during the SUNDIAL 1987 campaign. Two specific intervals of varying interplanetary magnetic field, which also include several substorms, have been identified for detailed study. The two intervals differed considerably in both the input of energy from the solar wind to the magnetosphere prior to the substorm expansion phase onset and the response during the expansion phase. One substorm can be represented by the classical picture of growth phase, expansion phase and recovery phase. The other, which occurred during an interval of weak energy input from the solar wind to the magnetosphere, was more complex, in particular during the expansion phase. Observations of the earth's magnetic field in the midnight sector provide the timing of the expansion phase onset of substorms which allow the separation of ionospheric effects due to changes in IMF and substorms. The primary ionospheric effect of a change in the IMF from positive B_z to negative B_z is an enhancement in the plasma flow magnitude. The response time of the ionospheric convection to each southward turning varies from 15 minutes near 1800 MLT to 30 minutes near 2100 MLT and closer to an hour near midnight. In both instances, a growth phase can be identified as an increase in ionospheric convection following a southward turning of the IMF. The overall length of each growth phase was similar, about 90 minutes, despite the different prevailing solar wind and IMF conditions. Furthermore this time is somewhat longer than previous observations. During one of the substorms, which consisted of several intensifications, there is evidence that the nightside flow reversal moved progressively to earlier local times in response to each substorm intensification.

14. SUBJECT TERMS	15. NUMBER OF PAGES
Ionospheric convection, Ionospheric substorms, Effects of IMF (Interplanetary magnetic field) Changes on the Ionosphere, Auroral oval, Disturbed ionosphere	16
	16. PRICE CODE

17. SECURITY CLASSIFICATION OF REPORT	18. SECURITY CLASSIFICATION OF THIS PAGE	19. SECURITY CLASSIFICATION OF ABSTRACT	20. LIMITATION OF ABSTRACT
UNCLASSIFIED	UNCLASSIFIED	UNCLASSIFIED	SAR

SF 298 (Cont'd)

Cont of Author Affiliations, Block 11

M. Lester [1], O. de la Beaujardière [2], J.C. Foster [3], M.P. Freeman [4*], H. Lühr [5], J.M. Ruohoniemi [6], W. Swider [7]

[1] Ionospheric Physics Group, Department of Physics and Astronomy, University of Leicester, Leicester, LE1 7RH, UK
[2] SRI International, Menlo Park, California 94025, USA
[3] MIT Haystack Observatory, Westford, MA 01886, USA
[4] Space and Atmospheric Physics Group, Blackett Laboratory, Imperial College, London, SW7 2AZ, UK
[5] *Institut für* Geophysik und Meterologie der Technischen Universität Carolo-Wilhelmina, D-38106 Braunschweig, Germany
[6] The Johns Hopkins University, Applied Physics Laboratory, Laurel, MD 20723-6099, USA
[7] Phillips Laboratory, Hanscom AFB, MA 01731, USA

Ann. Geophysicae 11, 556–571 (1993)

Annales Geophysicae

The response of the large scale ionospheric convection pattern to changes in the IMF and substorms: Results from the SUNDIAL 1987 campaign

M. Lester [1], O. de la Beaujardière [2], J.C. Foster [3], M.P. Freeman [4*], H. Lühr [5], J.M. Ruohoniemi [6], W. Swider [7]

[1] Ionospheric Physics Group, Department of Physics and Astronomy, University of Leicester, Leicester, LE1 7RH, UK
[2] SRI International, Menlo Park, California 94025, USA
[3] MIT Haystack Observatory, Westford, MA 01886, USA
[4] Space and Atmospheric Physics Group, Blackett Laboratory, Imperial College, London, SW7 2AZ, UK
[5] Institut für Geophysik und Meterologie der Technischen Universität Carolo-Wilhelmina, D-38106 Braunschweig, Germany
[6] The Johns Hopkins University, Applied Physics Laboratory, Laurel, MD 20723-6099, USA
[7] Phillips Laboratory, Hanscom AFB, MA 01731, USA

Received May 5, 1992; revised February 17, 1993; accepted March 26, 1993

Abstract. This paper reports multi-point observations of ionospheric convection made during the SUNDIAL 1987 campaign. Two specific intervals of varying interplanetary magnetic field, which also include several substorms, have been identified for detailed study. The two intervals differed considerably in both the input of energy from the solar wind to the magnetosphere prior to the substorm expansion phase onset and the response during the expansion phase. One substorm can be represented by the classical picture of growth phase, expansion phase and recovery phase. The other, which occurred during an interval of weak energy input from the solar wind to the magnetosphere, was more complex, in particular during the expansion phase. Observations of the earth's magnetic field in the midnight sector provide the timing of the expansion phase onset of substorms which allow the separation of ionospheric effects due to changes in IMF and substorms. The primary ionospheric effect of a change in the IMF from positive B_z to negative B_z is an enhancement in the plasma flow magnitude. The response time of the ionospheric convection to each southward turning varies from 15 minutes near 1800 MLT to 30 minutes near 2100 MLT and closer to an hour near midnight. In both instances, a growth phase can be identified as an increase in ionospheric convection following a southward turning of the IMF. The overall length of each growth phase was similar, about 90 minutes, despite the different prevailing solar wind and IMF conditions. Furthermore this time is somewhat longer than previous observations. During one of the substorms, which consisted of several intensifications, there is evidence that the nightside flow reversal moved progressively to earlier local times in response to each substorm intensification.

* *Present address:* British Antarctic Survey, High Cross, Madingley Road, Cambridge, CB3 0ET, UK
Correspondence to: M. Lester

1 Introduction

The magnetospheric substorm is the major mechanism for the release of energy from the magnetosphere into the nightside ionosphere. Initially the substorm was identified in ground-based auroral images and magnetometer data (Akasofu, 1968), but since the advent of in situ spacecraft measurements, in particular at geosynchronous orbit in the geomagnetic tail, the large scale nature of substorms has become more widely appreciated. Several review articles have covered a variety of aspects of substorm research (McPherron, 1979; Rostoker *et al.*, 1980, 1987; Baumjohann, 1988). Much of the work on magnetospheric substorms has centered upon the search for a model to explain the general nature of the phenomenon. At present, several models have been proposed (see review by Kan, 1990); the directly driven mechanism (Akasofu, 1980); the energy storage-release mechanism involving the formation of a near-Earth neutral line (Hones, 1979); the low-latitude boundary layer model (Rostoker and Eastman, 1987); and the thermal catastrophe model (Smith *et al.*, 1986, Goertz and Smith, 1989). Considerable controversy remains concerning which of the above most accurately represents the substorm and attempts to synthesis the various models are now being made (Lui, 1991).

The role of the magnetospheric substorm in coupling the magnetosphere and ionosphere is particularly important. One of the manifestations of this coupling is the high latitude ionospheric convection pattern. Ionospheric convection on the dayside is driven predominantly by reconnection between the interplanetary magnetic field (IMF) and the geomagnetic field as first proposed by Dungey, (1961). For southward IMF and under steady state conditions, open magnetic field lines move across the polar cap in an anti-sunward direction. These open field lines then reconnect in the geomagnetic tail and a return flow in the ionosphere is imposed on closed magnetic field lines. The resultant two cell, ionospheric convection pattern for southward IMF conditions has been well established and empirical models of the average convection pattern developed from both spacecraft observations (e.g. Heelis, 1984;

Heppner and Maynard, 1987) and ground based radar observations (e.g. Foster, 1983, Foster *et al.*, 1981; Waldock *et al.*, 1985). The convection pattern for northward IMF conditions is, as yet, not as well understood and may consist of three or four cells (Heelis, 1984) or two distorted cells (Heppner and Maynard, 1987).

Although these empirical models provide useful information on the average behaviour of ionospheric convection, they provide little information on the response times of convection to changes in the IMF or on the instantaneous convection pattern. Studies of the response of the dayside high latitude convection pattern to changes in the north-south, Z, component of the IMF have been undertaken with the EISCAT Polar experiment (Etemadi *et al.*, 1988; Todd *et al.*, 1988; Lockwood, 1991). In the noon local time sector, the magnitude of the convection flow increases a few minutes after the arrival of southward IMF at the subsolar magnetopause, but this lag increases to between ten and fifteen minutes at 0800 MLT and 1900 MLT (Etemadi *et al.*, 1988). Similar response times of the ionospheric convection near noon to changes in the Y component of the IMF have been found by Greenwald *et al.*, (1990) in simultaneous conjugate radar observations. The average response time between an IMF transition and the start of the convection reconfiguration was 8 minutes and the new convection pattern was achieved within 6 minutes of this reconfiguration onset. Although an increase in the strength of the convection flow in the dawn sector may occur up to fifteen minutes after a southward turning of the IMF, the boundary between the sunward and anti-sunward convection flows, often termed the polar cap boundary, has been seen to move equatorward in the pre-dawn sector some 4 to 12 minutes after a southward turning of the IMF (Lester *et al.*, 1990). Recent models of ionospheric convection (Siscoe and Huang, 1985; Moses *et al.*, 1987, 1989; Lockwood *et al.*, 1990) propose that the instantaneous convection pattern will be determined by the balance between reconnection rates at the dayside magnetopause and in the tail. If the former dominates then ionospheric convection will be strongest on the dayside; if the latter dominates then ionospheric convection will be strongest on the nightside. These models do not explicitly require substorms to be the primary source for the nightside convection, but it seems likely that they play a significant role. Furthermore, the onset of magnetospheric substorms is closely related to the IMF orientation at the magnetopause (e.g. Foster *et al.*, 1971).

In this paper we consider the response of the ionospheric convection in the post dusk and midnight sectors to changes in the IMF B_z component, as well as the effect of one isolated substorm and two weak substorms on ionospheric convection. This study is undertaken with the data set collected during the SUNDIAL 1987 campaign and, in particular, an extended run of the Incoherent Scatter radars at EISCAT, Sondrestrom Fjord and Millstone Hill. The SUNDIAL campaign of 1987 (Szuszczewicz *et al.*, 1993) lasted from May 29 to June 8 and during this interval the incoherent scatter facilities operated continuously from June 1 to June 5. Data from this latter period have also been used for the GISMOS campaign (Clauer *et al.*, 1989). The incoherent scatter systems measure a range of ionospheric parameters, but only the ion velocity perpendicular to the magnetic field in the F region and electron density in the E region will be presented here. This paper considers two specific intervals, one from 2200 UT on June 1 to 0400 UT on June 2, and the other from 1800 UT on June 2 until 2400 UT on June 2. Each interval contained at least one substorm, identified by data from the EISCAT magnetometer cross (Lühr *et al.*, 1984). The co-ordinates of the 7 stations in this network are given in Table 1. Each of the incoherent scatter radars operated a different programme which will be described as the data are discussed. Other data sets are available, but not shown, from the VHF coherent radar at Wick, originally part of SABRE (Nielsen *et al.*, 1983) and the HF coherent PACE radar at Goose Bay (Greenwald *et al.*, 1985). Although the HF and VHF systems operated

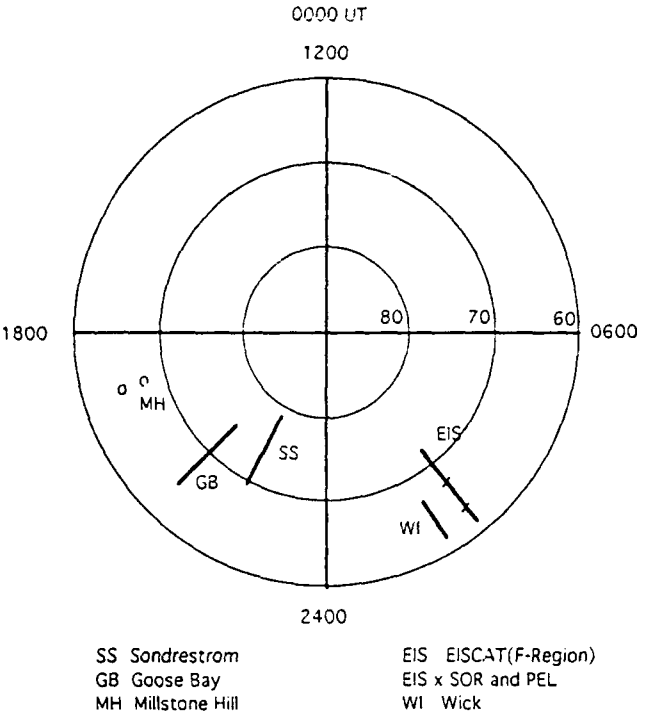

Fig. 1. Polar plot which shows the locations of the radar fields of view and magnetometer stations in invariant latitude and magnetic local time at 0000 UT.

Table 1. Locations of the stations of the EISCAT magnetometer cross

Station identifier	Geographic		Corrected geomagnetic	
	Lat	Long	Lat	Long
SOR	70.5	22.2	67.3	107.9
ALT	69.9	23.0	66.6	107.8
KAU	69.0	23.1	65.8	107.2
MUO	68.0	23.5	64.7	106.7
PEL	66.9	24.1	63.6	106.2
KIL	69.0	20.8	66.0	105.6
KEV	69.8	27.0	66.2	110.6

continuously they require the presence of plasma irregularities in the ionosphere to cause radar backscatter. Backscatter was detected by both systems during the first interval, but only on the Goose Bay system during the second. The location of all of the radar fields of view and the magnetometers at 0000 UT in invariant latitude and magnetic local time (MLT) are given in Figure 1 for reference. IMF and solar wind data were available from the IMP-8 spacecraft. The equatorward bounday of the auroral oval in the midnight sector during the intervals was estimated from particle data from the DMSP spacecraft (Gussenhoven *et al.*, 1981).

2 Interval 1 – 2200 UT 1/6/87 to 0400 UT 2/6/87

Interplanetary Conditions

The three GSM components of the IMF, B_x, positive towards the sun, B_y, positive to the east, and B_z positive northward, are plotted in panels a to c of Fig. 2. The data finish just before 0400 UT. During this interval the IMP-8 spacecraft was located 36 R_E upstream from the Earth with Y and Z GSM coordinates of $-6\ R_E$ and $-13\ R_E$ respectively. Prior to the interval, B_z was ∓ 7 nT from $\sim$2000 UT, B_y was positive from $\sim$1900 UT and B_x was mainly negative apart from two brief positive intervals, the last of which started at 2154 UT. Throughout interval 1, the B_y component of the IMF was positive apart from two periods, 2201 UT to 2213 UT and 0006 UT to 0048. The B_z component turned negative at 2222 UT and, apart from a brief interval, 2304–2308 UT, remained negative until 0000 UT. A second shorter interval of negative B_z occurred between 0039 UT and 0102 UT. One final period of southward IMF started at $\sim$0243 UT, when the B_z component became 0 nT, eventually turning southward at 0258 UT, and lasted until 0328 UT. The total field magnitude (data not shown) was about 10 nT for most of the interval apart from a twenty minute interval before 0100 UT when it reached 15 nT.

The solar wind speed (not shown) during this interval was fairly stable at 380 km s^{-1} until $\sim$0028 UT when there was a rapid increase to 420 km s^{-1}. A gradual decrease to 380 km s^{-1} at 0100 UT was followed by a steady increase to 440 km s^{-1} at $\sim$0200 UT. The number density in the solar wind (not shown) prior to this interval reached a value of $\sim$35 cm^{-3}, which is considerably higher than normal at Earth orbit (Bame *et al.*, 1968), at about 2000 UT, remaining at this level until 2200 UT, the start of the interval studied here. From then there was a gradual decrease until $\sim$0300 UT when it had reached a value of 6 cm^{-3}. There followed a sharp increase in density to between 10 to 12 cm^{-3} where it remained until $\sim$0143 UT, after which the density decreased to between 8 and 10 cm^{-3}. In summary, although the speed of the solar wind during this interval was typical, the density was rather higher than normal, particularly in the first couple of hours.

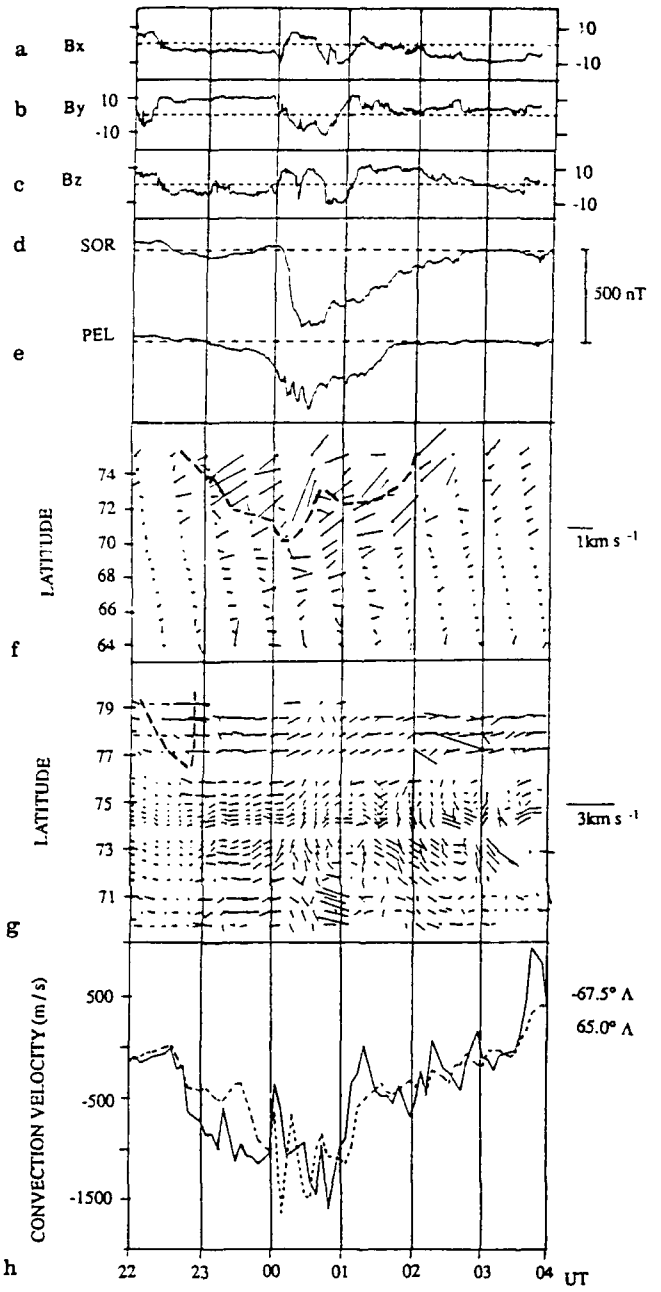

Fig. 2. Panels **a**–**c**. IMP-8 Interplanetary Magnetic Field (IMF) data from 2200 UT on 1 June 1987 (Day 152) to 0400 UT on 2 June 1987 (Day 153). The data are plotted in GSM coordinates. Panels **d**, **e**. The X (North-South) component of the magnetic field measured by SOR and PEL stations of the EISCAT magnetometer cross for the same interval. The scale is given to the right of the panel. Panel **f**. Tri-static measurements by the EISCAT radar of the ion velocity perpendicular to the magnetic field at 275 kms altitude for the same interval plotted against geographic latitude. The scale is given to the right of the panel. The dashed line represents the boundary between eastward and westward flow. Panel **g**. Estimates of the ion velocity perpendicular to the magnetic field by the Sondrestrom incoherent scatter radar for the same interval as a function of invariant latitude. The scale is given to the right of the panel. The dashed line represents the boundary between and westward flow. Panel **h**. Estimates of the east-west component of the ion velocity perpendicular to the magnetic field by the Millstone Hill incoherent scatter radar for the same interval at two invariant latitudes

The European sector

At the start of this interval the stations in the European sector are near magnetic midnight. The unfiltered X component (north-south) magnetograms from the northernmost, SOR, and the southernmost, PEL, stations of the EISCAT magnetometer cross (Fig. 2, panels d and e) indicate a substorm expansion phase onset just after 0000 UT (~0230 MLT) on 2 June. Negative X component bays occurred at all stations, consistent with an enhanced westward electrojet (eastward ion flow). The Z component bays (not shown) were negative at the two lowest latitude stations (MUO and PEL) and positive at the five higher latitude stations, indicating that the electrojet was centred at a latitude between MUO and KAU (64.7°Λ–65.8°Λ) (Kisabeth and Rostoker 1973, Rostoker *et al.*, 1980). The X component at each station reached its lowest value between 0020 UT and 0030 UT, and this was followed by the onset of the recovery phase of the substorm (Rostoker *et al.*, 1980). This latter phase lasted until about 0200 UT by which time the magnetic field at all stations had returned to its pre-substorm levels and the stations had moved towards dawn (~0430 MLT). The auroral break-up region of the substorm expansion phase is often identified with the western upward field-aligned current of the substorm current wedge. The longitudinal location of the current wedge cannot be unambiguously determined from the EISCAT magnetometer cross data. Data from the Lerwick magnetic observatory (not shown) for this interval indicate that the centre of the substorm current wedge, defined by the location where the mid-latitude Y component bay changes from positive to negative (McPherron *et al.*, 1973, Lester *et al.*, 1989), was west of Lerwick (geographic longitude ~0°E). Thus, the western field-aligned current of the substorm current wedge, and hence the auroral break-up region, would have been located to the west of Lerwick and also well to the west of the EISCAT magnetometer cross stations.

The time of the substorm expansion phase onset is usually identified to within a minute by the start of a Pi2 pulsation (Rostoker and Olson, 1979, Rostoker *et al.*, 1980). The EISCAT Cross magnetograms have been filtered in the Pi2 frequency range, 5–25 mHz, and the initial expansion phase onset identified at 0006 UT. Substorms often have secondary intensifications (Rostoker *et al.*, 1980) and there were subsequent Pi2 pulsations indicating such intensifications at 0016 UT, 0027 UT, 0038 UT, 0050 UT and finally during this expansion phase at 0116 UT. This last event was weak and only identified in the filtered Y component. Another Pi2 pulsation occurred at 0346 UT, but there were no strong concurrent bay signatures in the magnetometer data which suggests that the auroral break-up occurred well to the west of the EISCAT magnetometer cross longitude.

The EISCAT incoherent scatter facility operated the CP-3 programme (Baron, 1984) for the first 48 hours of the extended run followed by a 48 hour run of the UK programme Polar designed to study high latitude convection with high temporal resolution (van Eyken *et al.*, 1984). The two intervals discussed in this paper occurred during the CP-3 experiment in which the Tromsø transmitter scanned a range of latitudes making measurements in 17 different pointing positions, 16 of which were aligned approximately along a geomagnetic meridian. The remote sites at Kiruna and Södankylä followed the scan and intersected the transmitter beam at an altitude near 275 km, thus providing for tristatic measurements of the ion velocity at this altitude. The scan took just over 26 minutes to complete and each scan started on the hour or on the half hour UT. The first point in the scan was to the east of the geomagnetic meridian and has not been employed here.

The component of the tristatic ion velocities perpendicular to the magnetic field which were measured by the EISCAT radar during the 6 hour interval show several interesting features (Fig. 2, panel f). Between 1900 UT and 2130 UT (data not shown), the flow was predominantly south westward with magnitude ~700 ms^{-1} at latitudes above 72°N geographic latitude (~69°Λ) and westward with magnitude ~250 m s^{-1} at latitudes below 70°N (~67°Λ). The flows after 2130 UT were very weak (<400 m s^{-1}) at all latitudes and by 2230 UT the ion flow had turned eastward. An incursion of westward ion flow into the field of view from the north, was initially evident on the scan starting at 2300 UT (~0130 MLT). The boundary between westward and eastward flow moved equatorward to a minimum latitude of 67°Λ on the scan starting at 0000 UT (~0230 MLT). The last measurement of westward flow on this scan was made at 0011 UT, 5 minutes after the onset of the substorm expansion phase identified by the EISCAT magnetometer cross. On the scan starting at 0030 UT, the convection flow was predominantly eastward, apart from two measurements of equatorward flow at ~0035 UT and near 71°Λ. Another incursion of westward ion flow from the north then occurred on the following radar scan. The boundary between westward and eastward ion flow then retreated poleward at some time after 0136 UT and before 0200 UT, as did the equatorward boundary of the eastward convection. Notice also the general increase in flow magnitude between the scans which started at 2230 UT and 2330 UT. This increase in flow magnitude was particularly noticeable at the latitudes where the flow reversed direction.

Plotted in Fig. 3 are estimates of the electron density at 115 km altitude based upon the range corrected power and assuming $T_e = T_i$. If T_e was larger than T_i, which may have been the case during intervals of particle precipitation, then the actual electron density would have been higher than those estimated in Fig. 3. The assumption that $T_e = T_i$ is not critical in this study since no quantitative use is made of the electron density estimates. The threshold in electron density for the equatorward boundary of the auroral oval (see below) is purely illustrative of the change in latitude of the boundary during the interval of interest. At the altitude of 115 km and for the local time of the measurements, observations above about 1.0×10^{11} m^{-3} indicate particle precipitation. On the basis of this inferred particle precipitation, the auroral oval was located initially between 65°Λ and 68°Λ. However, there appeared to be an equatorward movement

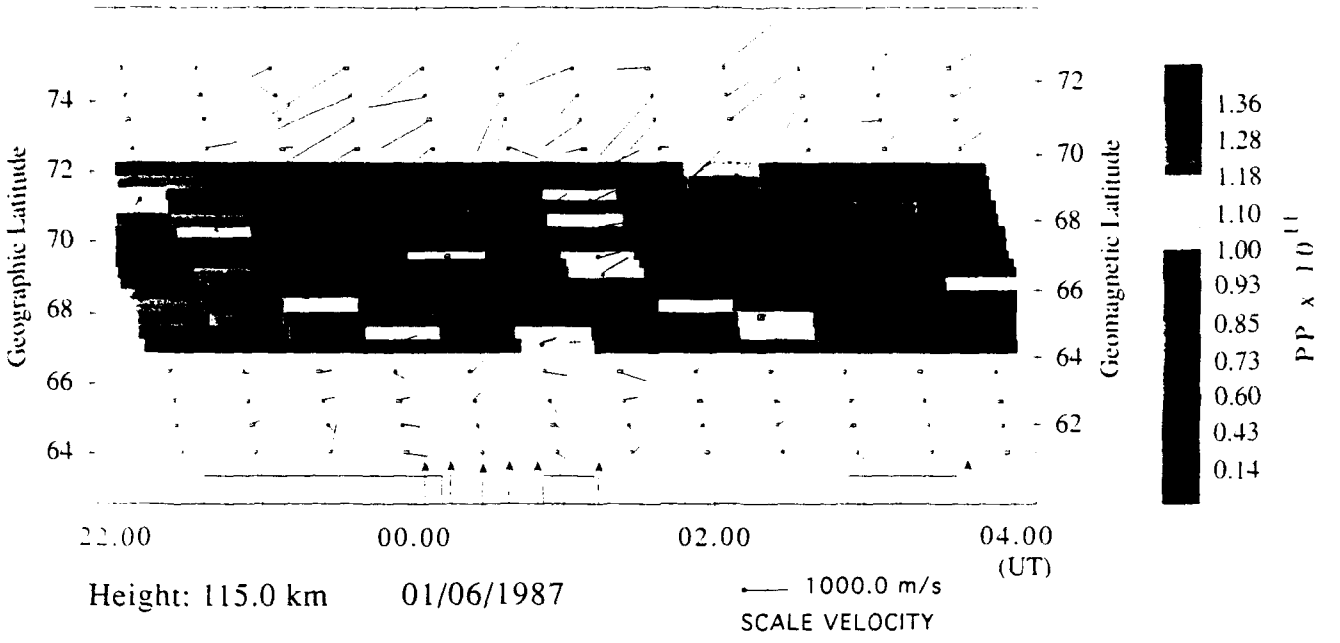

Fig. 3. Estimates of electron density measured by EISCAT at 115 km altitude as a function of time and latitude for the interval shown in Fig. 2. The colour code is given on the right of the panel. Overlaying the electron density measurements are the velocity vectors from Fig. 2f. The bars at the top (bottom) of the panel indicate the times of negative B_y (B_z) at the subsolar magnetopause. The vertical arrows at the bottom of the panel represent Pi2 pulsations.

between ~2237 UT and 2317 UT such that only the poleward edge of the aurora appeared within the radar field of view on the scan starting at 2300 UT. A poleward leap followed between ~2347 UT and 0009 UT, coincident with the substorm expansion phase onset. Between 0120 UT and 0148 UT the equatorward boundary of the particle precipitation again moved poleward, but this time more gradually. It moved from about 65°Λ at 0148 UT to about 67°Λ at 0342 UT, an average speed of ~30 m s^{-1}. The equatorward boundaries of particle precipitation and convection followed each other closely in this latter interval.

In the northern hemisphere, the equatorward edge of the auroral oval identified by the DMSP F6 spacecraft was located at ~66°Λ at ~0012 UT (~1950 MLT). The F7 spacecraft identified the equatorward edge of the oval at ~62.5°Λ at ~0005 UT (~0015 MLT). On the next passes of both spacecraft the equatorward edge had moved to 68°Λ at 1903 MLT (0152 UT, F6) and between 62°Λ and 64°Λ at 2350 MLT (0148 UT, F7), (this is hard to identify clearly because of the spacecraft track). The poleward motion of the equatorward edge of the pre-midnight auroral oval measured by DMSP during this interval was similar to that inferred in the post-midnight sector by the EISCAT E-region electron density measurements. However, the equatorward edge of the auroral oval in the midnight sector appeared to change little.

The Wick VHF coherent radar, which formed part of the SABRE system (Nielsen *et al.*, 1983), was operational throughout the campaign. Coherent backscatter occurred from 2320 UT (~0120 MLT) until 0135 UT (~0335 MLT), during which time the line of sight velocity was away from the radar, consistent with eastward convection flow and, thus, the return flow of the morning convection cell. The convection flows measured by EISCAT during the interval of coherent backscatter and at magnetic latitudes similar to the Wick measurements (62–67°Λ), were also eastward from 2320 to 0135 UT (Fig. 2, panel f). The SABRE backscatter intensity was fairly weak at first, <10 dB, but increased rapidly at ~2351 UT. This time coincided with an increase in the magnitude of the line of sight velocity to more than 500 m s^{-1} at ~65.5°Λ. This increase is consistent with EISCAT ion flow measurements where the flow magnitude increased after ~2300 UT and may represent the general expansion of the convection pattern due to the southward turning of the IMF at ~2223 UT, as will be discussed later. The peak intensity of coherent backscatter and maximum line of sight velocity, measured by the Wick radar occurred between 0000 UT and 0020 UT, the expansion phase of the substorm. There was a general decrease in the magnitude of the line-of-sight velocity from 0030 UT (~0230 MLT), consistent with EISCAT ion flow measurements, which were generally weaker on the scan starting at 0100 UT (~0330 MLT) at the lower latitudes, as well as the magnetometer data, which indicated the beginning of the substorm recovery phase at ~0030 UT.

The North American sector

Convection flow velocities are calculated from Goose Bay coherent radar data by fitting the line of sight velocity along 16 beams to a cosine relationship (Ruohoniemi *et al.*, 1989). During the interval of interest, the radar observed F-region backscatter at latitudes 69–71°Λ from

2346 UT (~2046 MLT) and relatively large westward flow velocities, >1 km s^{-1}, occurred for about 10 minutes. After this period only E-region backscatter, at latitudes $<68°\Lambda$, was present and during the interval 0000 UT (~2100 MLT) to 0020 UT (~2120 MLT) the convection was highly variable, both spatially and temporally, such that there is difficulty in fitting flow velocities to the data. A stable convection pattern was established, characterised by a strongly westward flow, at ~0025 UT in this E-region backscatter. A second distinct transition in the flow was a change to equatorward flow at 0100 UT (~2200 MLT) as the radar entered the region of the Harang Discontinuity and all backscatter had died away by 0155 UT. F-region backscatter returned at 0240 UT and from 0300 UT the flows were eastward and considerably stronger, occasionally larger than 1 km s^{-1}.

The operating mode of the Sondrestrom incoherent scatter radar for this interval was a modified World Day Mode (de la Beaujardiére *et al.*, 1987) which consisted of one elevation scan in the magnetic meridian and two pairs of positions at 30° elevation angle looking to the north and to the south. The two pairs extended the convection coverage obtained from the elevation scan such that the convection measurements were made between ~69.5°Λ and ~79°Λ. The elevation scan velocity vectors were obtained following a procedure in which the line-of-sight ion velocities at both E and F region heights were combined with a neutral atmosphere model to derive the ion velocity component perpendicular to the line of sight (de la Beaujardiére *et al.*, 1977). The ion velocity measurements by Sondrestrom (Fig. 2, panel g) indicate an incursion of eastward flow into the radar field of view from the north starting at ~2215 UT (~2015 MLT); the reversal in flow between eastward and westward flow moved steadily equatorward over the next 30 minutes reaching 72°Λ. Between 2245 UT and 2254 UT the flow reversal moved rapidly poleward and the flow subsequently became westward over the whole field of view and remained essentially so until ~0000 UT. At ~0010 UT there is evidence of a localised region of equatorward flow near 73°Λ, which extended to below 70°Λ on the following scan and later extended poleward, also eventually covering the complete latitude range by 0040 UT. After 0100 UT and until 0400 UT, the flows became rather irregular with predominantly westward flow at latitudes $>77°\Lambda$, equatorward and mainly eastward flow at ~75°Λ and below. The Sondrestrom operational mode described earlier made measurements of the E region electron number density between 71°Λ and 76°Λ. During this interval there was evidence of particle precipitation and auroral arcs with densities above 10^{11} m^{-3} at 125 km altitude between 0017 UT and 0032 UT and again from 0116 UT to 0140 UT. On both occasions the equatorward border of the precipitation continued beyond the radar field of view. The poleward edge was evident, occurring near 73°Λ in the first case and poleward of 76°Λ in the second.

The incoherent scatter radar at Millstone Hill operated a beamswinging programme similar to the UK EISCAT Polar experiment. The Millstone experiment pointed in two direction, on either side of magnetic north, and the convection velocities at positions along the magnetic meridian were computed from the line of sight velocities at the same latitudes along each beam with ~8 minute temporal resolution. The estimated east-west component of the ion velocity at 67.5°Λ (full line) and 65°Λ (dashed line) are given in Fig. 2, panel h. Prior to ~2230 UT (~1730 MLT) the east west flow measured by Millstone Hill at both latitudes was typically less than 100 m s^{-1}. However, after 2244 UT the flow increased rapidly to larger than 500 m s^{-1} at 2308 UT at 67.5°Λ and at about 2340 UT at 65°Λ. The zonal component of the flow at this time was westward. The largest flow at 65°Λ occurred at 0017 UT, where it was >1500 m s^{-1}; indeed for most of the interval from 0015 UT to 0100 UT the magnitude remained larger than 1 km s^{-1} at both latitudes. After this, however, the flow magnitude decreased rapidly. After 0113 UT the flow magnitude was less than 500 m s^{-1} and the east-west component steadily declined. The flow direction remained predominantly westward until 0336 UT, when there was a reversal to predominant eastward flow. This flow reversal occurred simultaneously at both 67.5°Λ and 65°Λ.

3 Discussion – interval 1

Estimate of the spacecraft-magnetopause time lag

Before discussing the effects of the IMF and substorms on the convection pattern during this interval, it is necessary to discuss the computation of the time lag from the IMP-8 spacecraft to the subsolar magnetopause. The knowledge of this time lag is important in order to separate changes in ionospheric convection which may be due to one of several causes, e.g. change in IMF orientation, solar wind pressure pulses or substorm effects. By removing this time lag, the time from the subsolar magnetopause to the ionospheric instrument, identified as ΔT_{MR} by Lockwood and Cowley, (1988), can also be estimated. The calculation employs results from a gas-dynamic model of the flow of the magnetized solar wind around the magnetosphere (Spreiter and Stahara, 1980). Time lags based upon this model have been utilised in several recent studies (Etemadi *et al.*, 1988, Freeman and Southwood 1988, Freeman *et al.*, 1990, Lester *et al.*, 1990).

The calculation assumes that the velocity of a fluid parcel in the solar wind upstream of the Earth's bow shock is unaccelerated and directed anti-sunward. Another assumption is that the measurement at the spacecraft is representative of a "phase front", which is at some angle, ϕ, to the Sun-Earth line. The front is assumed to be linear over a greater scale size than both the orthogonal spacecraft distance from the Sun-Earth line and the cross section of the magnetosphere (~40 R_E) (but see Rostoker *et al.*, 1983). The time taken for the phase front, travelling with the local solar wind velocity v_∞, to reach the subsolar bow show, τ_1, is given by

$$\tau_1 = \frac{(X-(1+\beta)\,D+L\tan\phi)}{v_\infty} \qquad (1)$$

where X is the geocentric upstream distance of the spacecraft, $(1+\beta)\,D$ and D are the geocentric distances to the

subsolar bow shock and magnetopause respectively and L is the orthogonal distance of the spacecraft from the Sun-Earth line. The time taken to traverse the subsolar magnetosheath is given by

$$\tau_2 = \frac{8\beta D}{v_x} \quad (2)$$

This value is deduced from the model of Spreiter and Stahara, (1980) which implies that the subsolar magnetosheath velocity falls approximately linearly from $v_x/4$ at the bow shock to approximately zero at the magnetopause. As discussed by Lester *et al.*, (1990), the expression for τ_2 is an approximation based upon the assumption that the phase front motion does not entirely stagnate in the subsolar region, but that magnetic reconnection or MHD waves affect the transport of information in the subsolar region. The value of β ranges from 0.20 to 0.25 (Spreiter and Stahara, 1980). The total lag from spacecraft to subsolar magnetopause is given by

$$\tau = \frac{(X + L\tan\phi + (7\beta - 1)D}{v_x} \quad (3)$$

The geocentric subsolar magnetopause D is given by (Beard, 1960)

$$D = \left(\frac{\alpha^2 B_{eq}^2}{2\mu_0 P_x}\right)^{1/6} R_E \quad (4)$$

where B_{eq} (= 31 000 nT) is the equatorial magnetic field strength, μ_0 is the permeability of free space and P_x is the upstream dynamic pressure of the solar wind. The geometrical field compression factor, α, can range from 2 to 3 (Freeman *et al.*, 1990).

Taking account of the various values of density and velocity during interval 1 and assuming $|\phi| < 45°$ we find that the lag varied from 12 ± 5 minutes at the start of the interval to 10 ± 4 minutes at the end. The variability would be reduced by some 2 minutes if the phase front normal is restricted to being tilted in the X-Y GSM plane.

Effect of reversal of IMF B_y on nightside ionospheric convection

The control on the nightside ionosphere convection pattern exerted by the IMF can be divided into two major effects: asymmetry of the ionospheric convection pattern due to the azimuthal component of the IMF, B_y; the change in convection flow magnitude due to changes in the north-south component, B_z. A southward turning of the IMF can also be regarded as the onset of the substorm growth phase (McPherron, 1979) and this is discussed later. There is observational evidence for significant differences in the average nightside ionospheric convection for different signs of the B_y component (de la Beaujardière *et al.*, 1986, Foster *et al.*, 1986). The average flow direction measured by Sondrestrom between 1800 MLT and 0200 MLT is predominantly westward under positive B_y conditions compared with eastward at latitudes above 70 °Λ for negative B_y conditions. Many models of ionospheric convection (e.g. Friis-Christensen *et al.*, 1985; Reiff and Burch, 1985; Heppner and Maynard, 1987) do not reproduce all of the features noted in the averaged convection pattern measured by Sondrestrom on the nightside. Another nightside asymmetry in the convection flow due to differing B_y conditions was reported by Burrage, (1988) who demonstrated that the nightside flow reversal measured by SABRE occurs about an hour earlier when B_y is positive. This observation has been subsequently supported by observations showing the movement of the nightside flow reversal, or Harang discontinuity, to later local times in the southern hemisphere when IMF B_y became less negative (Dudeney *et al.*, 1991).

During interval 1 the IMF B_y component was predominantly positive with two excursions of negative polarity, 2201 UT–2213 UT and 0006 UT–0048 UT, at IMP-8 (~2213–2225 UT and 0018–0100 UT at the subsolar magnetopause). Neither time is particularly well suited for investigating the effect of B_y on ionospheric convection in the post dusk local time sector or the response time of changes in B_y. The former, apart from being brief, only 12 minutes, occurred during an interval of positive B_z and both changes of B_y polarity were gradual rather than steplike. Based upon the average results of de la Beaujardière *et al.* (1986), a change of B_y from positive to negative would result in a change of flow direction from westward to eastward in the 18–02 MLT sector and at latitudes greater than 70 °Λ. Such a change in flow direction was first seen at 2225 UT. The interval of eastward flow then lasted for at least 20 minutes, changing at all latitudes between 2244 UT and 2254 UT, much longer than the 12 minute interval of negative B_y polarity. Despite the brief interval of negative B_y, the interval when B_y was less than 10 nT did last for 30 minutes. The exact relationship between the incursion of eastward flow and the change in B_y is unclear in this case.

The effect of the second change to negative B_y is difficult to assess since it ocurred just after the expansion phase onset. There were no similar incursions of eastward flow at latitudes >77 °Λ during the second interval of negative B_y. The flow after the expansion phase of the substorm, i.e. from about 0100 UT onwards, was typical of the positive B_y conditions that then prevailed.

Although the general features of flow measured by the EISCAT CP-3 programme can be related to the IMF, the response time of the ionospheric convection to changes in the IMF cannot be estimated accurately because of the relatively long scan time, 30 minutes. An incursion of westward ion flow which was first observed at ~72 °Λ on the scan starting at 2300 UT (~0130 MLT) is consistent with the averaged ion flows at Sondrestrom for positive B_y at an MLT of ~0130 MLT (de la Beaujardière *et al.*, 1986) which indeed was the situation during this time. From 2300 UT to 0300 UT this westward flow was absent on only two scans, those starting at 0030 UT (~0300 MLT) and 0200 UT (~0430 MLT). In the former, the lack of westward flow could have been due to either the B_y component turning negative at 0019 UT at the subsolar magnetopause, which lasted until 0100 UT, or the B_z component turning positive at ~0015 UT, or the substorm that occurred at 0006 UT. Westward flow was not present from 0300 UT (~0530 MLT), even though B_y remained positive. This, however, is still consistent with earlier Son-

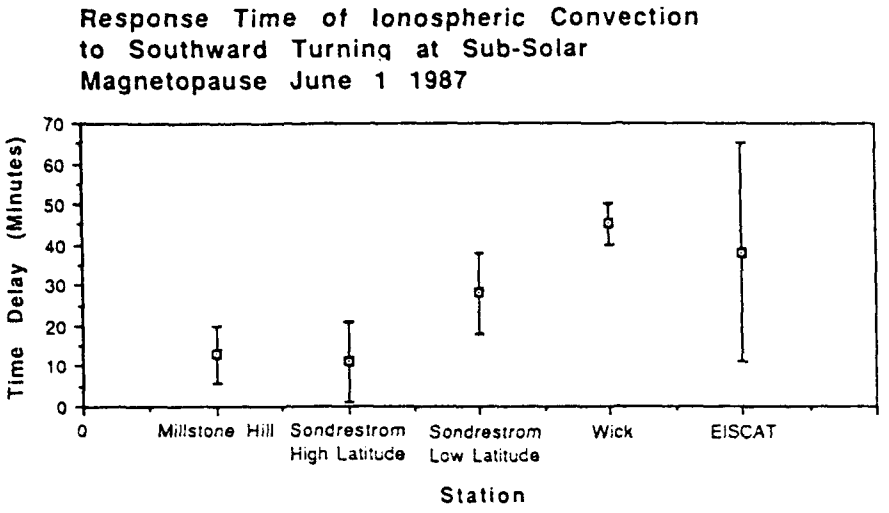

Fig. 4. The estimated response time of the ionospheric convection at four stations to a change of B_z from positive to negative at the sub-solar magnetopause

drestrom observations for positive B_y (de la Beaujardière *et al.*, 1986) since the boundary between westward and eastward flow was moving to successively higher latitudes between 0200 and 0400 MLT.

The substorm growth phase

The substorm growth phase has been a topic of some controversy since it was first proposed (McPherron, 1970), in particular the causative nature of the growth phase within the overall substorm process remains unclear. Foster *et al.*, (1971) demonstrated that the AE index, which estimates the maximum auroral magnetic disturbance at any local time, begins to increase at the time of the IMF B_z southward turning and that the average duration of this growth phase is 80 minutes. Describing the features of the growth phase McPherron (1979) noted that it began with a southward turning of the IMF leading to an increase in the magnetic flux in the geomagnetic tail.

During interval 1, B_z turned southward at ~2222 UT at the spacecraft after an interval of over 2 hours of northward IMF. This reversal reached the magnetopause some 7–17 minutes later. At latitudes $74° < \Lambda < 76°$ Sondrestrom measured a clear increase in flow magnitude between 2240 UT and 2250 UT and at $\Lambda < 73°$ between 2257 UT and 2307 UT. This would imply a time lag of 1–21 minutes at high latitudes and 18–38 minutes at lower latitudes for the effect of the change in B_z at the subsolar magnetopause to be transmitted to these latitudes and local time. No clear onset to the increase in flow magnitude can be identified at latitudes $> 77°\Lambda$, although between 2245 UT and 2255 UT the convection reversed from eastward to westward.

The ionospheric convection flow magnitude measured by Millstone Hill started to increase between 2244 UT, when the flow at $67.5°\Lambda$ was 202 m s^{-1}, and 2249 UT, when the flow was 441 m s^{-1}. Eventually the flow stabilised at ~800 m s^{-1} at 2258 UT. These observations indicate a lag of between 5 and 20 minutes for the effect of the southward turning of the IMF to have reached this local time sector (~1800 MLT), with a further 10 minutes for the new convection magnitude to be established. This latter time scale may not correspond to an intrinsic response time of the magnetospheric system, but rather a response to an increasingly negative B_z component over the 10 minute interval after the polarity reversal.

Estimating accurately a time lag for the onset of enhanced convection in the EISCAT local time sector due to the southward turning is difficult because of the time resolution of the EISCAT scan. However, at latitudes $61° < \Lambda < 68°$ the magnitude of the ion flow within the EISCAT field of view increased between the scans (2249 ± 07) UT and (2319 ± 07) UT, but based upon the measurements at higher latitudes this increase probably occurred between (2305 ± 02) UT and (2335 ± 02) UT. Thus the lag was between 10 and 65 minutes. The Wick observations of coherent backscatter did not start until 2320 UT and then initially only at low intensity. This fact implies that the effect of the southward turning of the IMF takes of the order 40–50 minutes to reach the nightside ionosphere at these latitudes and local time. No substorms occurred before 0000 UT, which implies that the increase in flow magnitude at EISCAT and the onset of backscatter at Wick are most likely to have been due to the southward turning of the IMF.

These observations imply that there was a lag in the effect of the southward turning to be transmitted to the ionosphere, which is summarised in Fig. 4, where the response time at the 4 stations is plotted with the western most station on the left and the eastern most station on the right. The MLT range in the figure is ~1800 MLT at Millstone Hill to ~0200 MLT at EISCAT. Although there are two estimates from different latitude regions at Sondrestrom no account has been taken of the different latitudes of the stations. These observations extend the previous work which identified the response time of ionospheric convection in the dusk sector to a southward turning of the IMF (Etemadi *et al.*, 1988; Todd *et al.*, 1988) into the midnight sector.

A second point regarding the response to the southward turning of B_z concerns the overall length of the growth phase of the substorm in interval 1, from south-

ward turning to the expansion phase onset. Based upon the timing of the southward turning at the subsolar magnetopause during the first interval, i.e. 2234 UT ± 5 minutes, the growth phase of the isolated substorm lasted between 87 and 97 minutes. Some studies, which have attempted to measure the response of the overall magnetospheric system to the energy input from the solar wind, have demonstrated that this response is characterised by two different timescales (Bargatze *et al.*, 1985). Each of these two response times, ~20 minutes and ~60 minutes, are dominant under different conditions; the shorter response time for strongly active conditions, minimum AL index of −1250 nT, and the longer response time for moderately active conditions, minimum AL index of −600 nT. The minimum AL index for this substorm interval was ~ −500 nT, indicative of moderate magnetic activity. In contrast, a computer simulation study (Kan *et al.*, 1988) predicts that auroral substorm onset occurs about 40 minutes after a southward turning of the IMF. In this simulation, however, two necessary conditions for substorm expansion phase onset are (1) the polar cap potential must exceed a certain value and (2) the nightside convection reversal region must overlap with the poleward gradient of the diffuse auroral conductance in the ionosphere in the midnight sector.

In summary, for the substorm in interval 1 there are two separate aspects of the response of the magnetospheric system to the southward turning of the IMF. Firstly, the increase in convection flow magnitude, in response to the southward turning of the IMF, is indicative of the growth phase and represents a "directly driven" component. The response time is variable, depending upon the local time and latitude of the radar field of view, ranging from 5–20 minutes at Millstone Hill to 41–51 minutes at Wick. The second aspect is the overall length of the growth phase which is 90 minutes and is, longer than either the second response time of Bargatze *et al.*, (1985) or the prediction of Kan *et al.*, (1988), but in keeping with the statistical average determined by Foster *et al.*, (1971). Furthermore, our study clearly shows that enhanced sunward convection occurred in both the evening and morning convection cells during the substorm growth phase.

Expansion phase

The expansion phase of the substorm during interval 1 began at 0006 UT based upon the first Pi2 observed by the EISCAT cross magnetometer. Based upon magnetometer data from Lerwick the westward edge of the substorm current wedge (McPherron *et al.*, 1973) was to the west of the Lerwick meridian. Data from the Greenland magnetometer network (E. Friis-Christensen, personal communication, 1992) indicate a substorm enhanced westward electrojet centred at ~71°Λ at 0012 UT on both the west and east chains of the network. Thus the westward edge of the substorm current wedge at expansion phase onset was located between the Lerwick meridian and the eastern meridan of the Greenland chain and was followed by a westward expansion of the electrojet. Measurements of the E-region electron density at EISCAT and Sondrestrom indicate a poleward leap of the auroral particle precipitation at EISCAT at the time of the expansion phase onset and an enhancement of the E-region electron number density below 74°Λ at Sondrestrom from 0016 UT until 0032 UT. The convection at Sondrestrom below 73°Λ in the 2200 MLT sector turned predominantly equatorward between 0005 UT and 0015 UT. Unfortunately, there were two changes in the IMF near the expansion phase onset: B_z turned positive at 0000 UT (~0012 UT at the subsolar magnetopause); and B_y turned negative at 0006 UT (~0018 UT at the subsolar magnetopause). It is unlikely that the northward turning resulted in this flow change in the Sondrestrom field of view. It is hard to understand why a change to northward B_z component would result in equatorward flow at the lowest latitudes in the field of view alone. If the convection pattern were to contract due to the northward turning, the flow would be expected to turn poleward (e.g. Lester *et al.*, 1990). Such a poleward contraction of auroral zone convection may have occurred at EISCAT ~30 minutes after substorm expansion phase onset, although the timing is inaccurate because of the nature of the EISCAT scan. The region of most intense particle precipitation moved poleward between ~0040 UT and 0110 UT, coincident with the brief northward turning of the IMF between 0000 UT and 0030 UT, after taking account of the delay time between IMP-8 and the subsolar magnetopause and the response time of the magnetosphere. A more protracted poleward retreated occurred later during the sustained northward IMF interval. There is no evidence from the average convection flow for either sign of B_y (de la Beaujardière *et al.*, 1986) to suggest that this equatorward flow was due to the change in the B_y component, since for both signs of B_y the averaged measurements imply westward flow in this local time sector at the latitudes below 73°Λ. Average convection patterns, however, can be misleading when discussing individual case studies, especially at local times when the B_y imposed asymmetry is most significant, i.e. in the cusp and Harang discontinuity local time. However, the timing of the change in B_y suggests that the equatorward flow was more likely a result of the substorm expansion phase onset at 0006 UT. The flow direction at this MLT was predominantly out of the polar cap with the flow in the northern latitudes towards earlier local time. Thus it seems that the nightside equivalent of the dayside merging gap, i.e. the site of nightside reconnection probably mapped into this particular part of the ionosphere during this substorm.

Goose Bay observations at ~1 hour local time earlier than those at Sondrestrom were somewhat patchy between 0000 UT and 0020 UT, but after this there was an interval of E region backscatter at latitudes <68°Λ with line of sight velocities consistent with westward flow. The latitudes of the Goose Bay observations were equatorward of the Sondrestrom field of view. This further confirms, therefore, that the equatorward turning of the flow observed by Sondrestrom was associated with the Harang discontinuity. The rapid appearance of the flow reversal at 0100 UT, rather than a gradual reversal in flow, suggests that this was due to the expansion phase onset.

East of the break-up region the ionospheric convection exhibited two separate changes. The EISCAT scan starting at 0000 UT (~0230 MLT) retained the westward flow at high latitudes. The first observation of eastward flow occurred at ~0013 UT, 7 minutes after the expansion phase onset, at 66° Λ. It would seem therefore that there was little immediate effect on the ion convection due to the substorm at the higher latitudes. At Millstone Hill westward convection at 65° Λ was enhanced to >1 km s^{-1} throughout the substorm, while a lesser response was observed at higher latitude. The enhanced westward electrojet identified in the EISCAT magnetometer data occurred at latitudes <69° Λ, i.e. where the ion flow was eastward on the EISCAT scan. On the scan starting at 0030 UT (~0300 MLT), the flow was predominantly eastward and this would appear consistent with both a B_y sign change and perhaps the contraction of the polar cap boundary on the nightside due to substorm activity as previously reported (Clauer *et al.*, 1989; Lester *et al.*, 1990). The polar cap boundary in these earlier studies was identified as the boundary between eastward (sunward) flow and westward (antisunward) flow. Assuming the same definition, then the polar cap boundary moved poleward from ~67° Λ to above 72° Λ in a maximum of 19 minutes, a minimum poleward speed of ~500 m s^{-1}, which is consistent with the values of Clauer *et al.*, (1989) and Lester *et al.*, (1990) who estimated poleward velocities of the polar cap boundary of ~300 m s^{-1} and 2000 m s^{-1} respectively. However, in these studies the effect of the sign of B_y was not considered. In the one case (Clauer *et al.*, 1989) the IMF was unknown and in the other (Lester *et al.*, 1990) the B_y component was ~0 nT.

There remains a question over the nature of the triggering mechanism of the onset of the expansion phase. The mechanisms can be divided into those external to the magnetosphere, e.g. changes in the orientation of the IMF (Rostoker *et al.*, 1983), or those internal to the magnetosphere, e.g. plasma instabilities in the magnetotail (Lui *et al.*, 1990). There is considerable evidence (e.g. Caan *et al.*, 1977; Pellinen *et al.*, 1982; Rostoker *et al.*, 1983) that a northward turning of the IMF can lead to a release of the energy stored in the magnetotail during the preceding interval of southward IMF. The northward turning of the IMF at 0000 UT may have been the trigger for the expansion phase onset at 0006 UT. The time lag from IMP-8 to the magnetopause, ~12 minutes, would suggest that this is unlikely. However, as mentioned earlier, the interval of northward IMF between 0000 UT and 0030 UT is coincident with an interval when the region of particle precipitation observed by EISCAT moved poleward.

Recovery phase

The onset of the recovery phase can be defined for high latitude magnetometers equatorward of the westward electrojet and east of the auroral break-up by a poleward leap of the westward electrojet and of energetic particle precipitation (McPherron, 1979). The poleward leap in the electrojet results in an increase in the magnitude of both H and Z components at stations originally equatorward of the electrojet centre (Rostoker *et al.*, 1980). Based upon data from the EISCAT cross magnetometer the earliest time the recovery phase could have started was 0025 UT. This time was well before the last Pi2 pulsation of this particular substorm, 0116 UT, suggesting that either the recovery phase did not in fact finally start until after 0116 UT, or there was some residual activity during the initial stages of the recovery phase. Based upon the radar data, the onset of the recovery phase occurred between 0100 UT and 0130 UT. A sudden decrease in the convection strength was observed at ~0100 UT at Millstone Hill and there was a significant poleward jump in the eastward convection and electron precipitation at ~0130 UT at EISCAT, coincident with the largest single increase in the H component on the EISCAT cross magnetometer. This and other similar convection and precipitation changes are attributable to northward IMF turnings with ~30 minute lag. Based upon the magnetometer data from the post midnight sector the recovery phase lasted until ~0200 UT which means that the whole isolated substorm lasted about 3.5 hours. Note, however, that throughout the recovery phase the ionospheric flows estimated by Sondrestrom remain strong.

4 Interval 2 – 1800 UT 2/6/87 – 2400 UT 2/6/87

Interplanetary conditions

The IMF, as measured by IMP-8, which was located at GSM coordinates X ~ 36 R_E, Y ~ 6 R_E and Z ~ −16 R_E, was remarkably steady during the second interval as well as being aligned more or less radially towards the Earth (Fig. 5). The total magnetic field (not shown) remained near 5 nT throughout the interval. The B_x component (Fig. 5, panel a) was about −3 nT throughout, apart from a brief interval between 2050 UT and 2110 UT, when all three IMF components changed. The B_y component (Fig. 5, panel b) was in general close to zero or just slightly negative apart from the intervals 1800 UT to 1840 UT and 2004 UT to 2110 UT. The B_z component (Fig. 5, panel c) was positive at the start of the interval but approached 0 nT at about 1840 UT and remained so until 2050 UT. After this B_z remained positive apart from an interval between 2130 UT and 2142 UT, at which time it became ~0 nT until 2305 UT. The solar wind speed never exceeded 460 km s^{-1} during the whole of the second interval. At the start of the second interval, the solar wind speed was ~440 km s^{-1} and by 2400 UT ~420 km s^{-1}, the lowest value of the interval. The number density was much lower than in the previous interval, ranging from 2 to 4 cm^{-3}. At ~2040 UT the speed increased from 420 to 460 km s^{-1}. This increase occurred at the same time that the density increased from 2 to 4 cm^{-3}, and just before the change in the IMF orientation (2050 UT to 2110 UT). At the start of the interval, based upon the solar wind velocity and density, the time lag from IMP-8 to the subsolar magnetopause was 11 ± 5 minutes and at the end 10 ± 5 minutes.

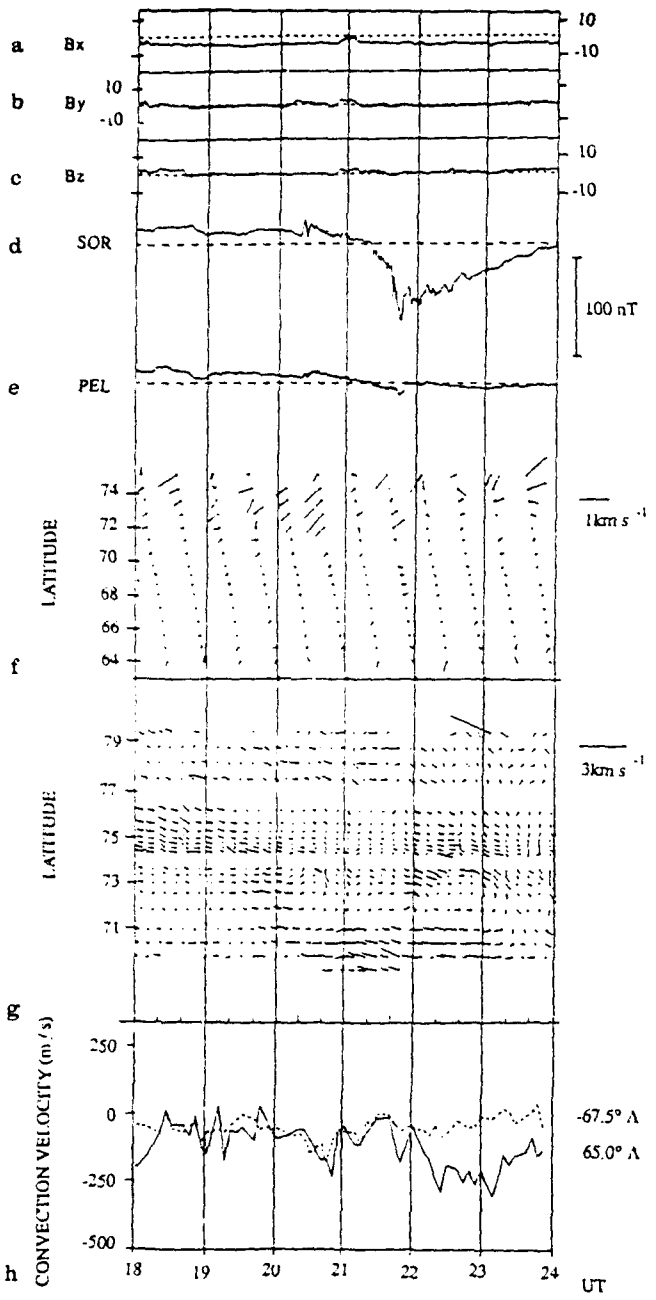

Fig. 5. Panels **a**–**c**. Interplanetary Magnetic Field data from 1800 UT on 2 June 1987 (Day 153) to 2400 UT on 2 June 1987 (Day 153). The data are plotted in GSM coordinates. Panel **d**, **e**. The X (North-South) component of the magnetic field measured by SOR and PEL stations of the EISCAT magnetometer cross for the same interval. The scale is given to the right of the panel. Panel **f**. Tristatic measurements by EISCAT of the ion velocity perpendicular to the magnetic field at 275 km s^{-1} altitude for the same interval. The scale is given to the right of the panel. Panel **g**. Estimates of the ion velocity perpendicular to the magnetic field by the Sondrestrom incoherent scatter radar for the same interval. The scale is given to the right of the panel. Panel **h**. Estimates of the east-west component of the ion velocity perpendicular to the magnetic field by the Millstone Hill incoherent scatter radar for the same interval for two latitudes.

The European sector

The magnetic activity during the second interval was quieter than the previous one and this is illustrated by comparison of the X component data from SOR and PEL of the EISCAT cross magnetometer for the second interval (Fig. 5, panels d and e respectively) with those in Fig. 2, panel d and e (note the different scales in the two figures). The maximum variation in interval 2 was less than 100 nT at all of the stations compared with at least 300 nT in the first interval. There were two separate periods of Pi2 wave activity, one starting at 2019 UT and the other starting at 2118 UT. It is unclear whether this activity represents one overall substorm expansion phase or two different expansion phases as will be discussed below. The first period of Pi2 wave activity consisted of up to three intensifications, identified in filtered data by Pi2 pulsations. There was a weak eastward electrojet (small positive X component bays, and positive Z component bay at SOR and negative Z component bays a KAU and MUO) at the time of the first Pi2 pulsation. This weak eastward electrojet implies that the auroral break-up associated with this expansion phase onset was to the east and/or poleward of the EISCAT magnetometer cross. Simultaneously with the second interval of Pi2 wave activity the Harang discontinuity swept over the magnetometer stations from east to west, evident from the polarity change of the X component at 2119 UT. This break-up obviously also started to the east of our network. Subsequent intensifications occurred at 2124 UT, 2131 UT and 2136 UT (again identified by Pi2 pulsations) and a magnetic bay was evident at the time of the last of the Pi2 pulsations. The signs of the bays in both H and Z components at the various EISCAT magnetometer cross stations, although small, suggest that there was a weak, substorm enhanced, westward electrojet centred between the stations SOR and ALT (67.3 °Λ and 66.6 °Λ).

The EISCAT ion velocity measurements (Fig. 5, panel f) indicate that the convection was very weak within the EISCAT field of view for much of the interval. Starting with the scan which began at 1830 UT (~2100 MLT), there was a gradual equatorward incursion of westward and equatorward flow, although the magnitude of the flow was in general less than 500 m s^{-1}. At 1936:40 UT and 1938:00 UT the flow was poleward at two positions, but apart from these two measurements, the flow remained westward at latitudes >67 °Λ until the scan starting at 2100 UT (~2330 MLT). After 2100 UT the flow became ill defined and highly variable, remaining so until 2300 UT (~0130 MLT) when the flow at latitudes above 70 °Λ was eastward.

The range corrected returned power at 115 km overlays the F region ion velocity measurements in Fig. 6. There were two intervals of particle precipitation both of which were related to Pi2 wave activity identified by the arrows. The first was observed by the radar only on the scan starting at 2030 UT and over the latitude range from 68 °Λ to 69 °Λ and the time interval 2032:20 UT to 2036:40 UT. The second was more extensive both in latitude and in time. The first indication of precipitation was at 2138 UT at a latitude of 67 °Λ and continued until

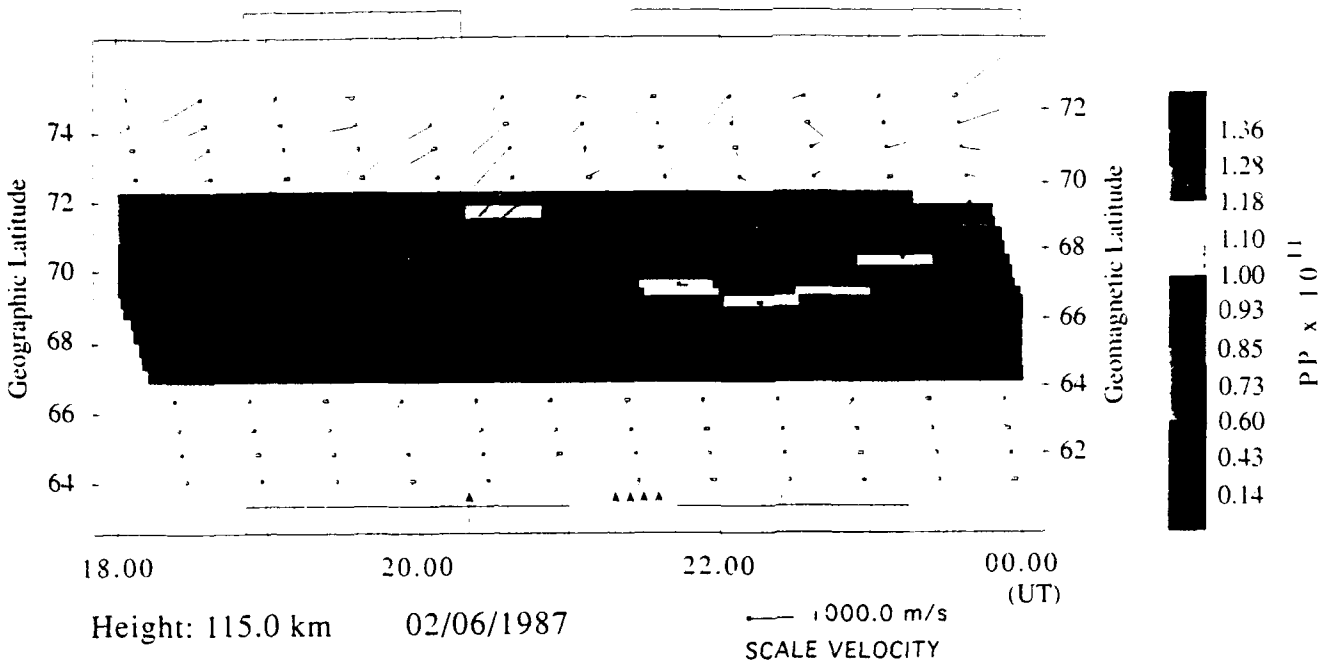

Fig. 6. Estimates of electron density measured by EISCAT at 115 km altitude as a function of time and latitude for the interval shown in Fig. 5. The colour code is given on the right of the panel. Overlaying the electron density measuremets are the velocity vectors from Fig. 5f. Bars at the top and bottom of the panel represent intervals of negative B_y and $B_z \leq 0$ nT respectively and the arrows represent the times of Pi2 pulsations.

2145 UT at 67 °Λ. On the following scan, the precipitation covered the latitude range from 66 °Λ to 69 °Λ and then on each of the following scans the equatorward boundary of the precipitation moved poleward. The relative lack of precipitation during the first interval of Pi2 wave activity is consistent with the view that the auroral break-up associated with this expansion phase was poleward and to the east of the magnetometer longitude. The onset of the second interval of precipitation was coincident with the final Pi2 pulsation, which was also the only Pi2 to have an associated bay at the EISCAT longitude.

The American sector

Although coherent backscatter was first observed by the Goose Bay radar during the second interval at ~2110 UT (~1810 MLT), it was not until ~2140 UT (~1840 MLT) that the flows became sufficiently well ordered that vector flow measurements could be made. The westward flow estimated after 2140 UT occurred over a limited latitude range between 71 °Λ and 73.5 °Λ until ~2235 UT (~1935 MLT) when the backscatter ceased. The backscatter did return at 2220 UT, continuing until 0140 UT, with the convection initially being westward, although the flow increased considerably after 0020 UT.

The convection flows measured by the Sondrestrom radar are somewhat complex (Fig. 5, panel g). At 1800 UT the flows were relatively weak, typically < 500 m s^{-1}, and predominantly westward. From ~1920 UT there was an incursion of eastward flow at high latitudes which moved equatorward reaching 77 °Λ until ~2005 UT when the flow at all latitudes returned to westward. Furthermore, as this eastward flow moved equatorward the flow magnitude at latitudes below 73 °Λ began to increase. After 2020 UT there was evidence for a localised band of flow with significant equatorward component between 71 °Λ and 73 °Λ. At latitudes below 71 °Λ the flow was westward and typically > 500 m s^{-1}; at latitudes above 73 °Λ the flow was also westward but typically < 500 m s^{-1}. The convection remained like this until about 2140 UT when the flow at latitudes above 71 °Λ became eastward with significant equatorward component at latitudes above 77 °Λ. The flow at all latitudes became predominantly equatorward after 2320 UT.

The convection flows measured by Millstone Hill at the two latitudes 67.5 °Λ and 65 °Λ (Fig. 5, panel h) were considerably weaker in this interval than in the first (Fig. 2, panel h). At 65 °Λ the flow magnitude (not shown) was less than 150 m s^{-1} throughout the whole interval, although the direction was predominantly westward. There were, however, stronger flows at 67.5 °Λ, although the flow was larger than 300 m s^{-1} only between 2215 UT and 2314 UT, peaking at 450 m s^{-1} at 2220 UT. The direction was westward throughout the second interval.

5 Discussion – interval 2

The IMF during the second interval was remarkably steady, weak, ~5 nT, and polarised predominantly in the GSM X direction. Furthermore, any changes in the IMF were very small. During the second interval, therefore, we

concentrate primarily on the substorm activity with some reference to the B_z component. The second interval contained two periods of Pi2 wave activity which had relatively weak effects on the planetary activity identified by the Kp index. However, the pulsations identify at least one substorm expansion phase, and there was enhanced particle precipitation in the European sector coincident with the wave activity.

The substorm growth phase

We again consider two aspects of the response to a change in B_z, i.e. the response at each station and the overall length of the growth phase. The ionospheric response to the changes in orientation of B_z during the second interval is much harder to quantify because the B_z component was truly negative only for a short period of time (2140–2152 UT at the subsolar magnetopause), although there are two long intervals where B_z was approximately 0 nT, ~1850 to 2100 UT and 2152 UT to 2315 UT at the subsolar magnetopause. At Sondrestrom, the only evidence of an increase in the convection flow magnitude in response to the change of B_z to 0 nT was seen at latitudes below 73°Λ, at about 1920 nT at 73°Λ and ~1950 UT at 70°Λ. There is no evidence of a specific time when the flow increased in magnitude in response to the southward turning of B_z at 2140 UT. This was probably because the southward turning occurred during a substorm expansion phase. At Millstone Hill there was no response to the change of B_z to 0 nT, but there was an increase in flow magnitude after 2200 UT in response to the southward turning at 2140 UT. At EISCAT there was no response to either period of $B_z \leq 0$ nT. Thus, the response time appears to be between 30 to 60 minutes at Sondrestrom, depending upon latitude, and >20 minutes at Millstone Hill, both of which are longer than the corresponding response time at these stations during interval 1, when they were at a later MLT.

Prior to the initial expansion phase onset at 2019 UT, there was no southward turning of the IMF although the IMF B_z component did change from ~3 nT to 0 nT at 1851 ± 5 UT at the subsolar magnetopause. Taking this change as the onset of the growth phase we find an overall length of the growth phase of between 81 and 91 minutes. The minimum value of the AL index during the first interval of Pi2 wave activity was only ~ −40 nT at 2040 UT. The small values of AL should not be unexpected. It is probable that the polar cap was very small throughout this growth phase because of the weak energy input from the solar wind. This small polar cap would imply that the electrojets, to which the AL index is sensitive, were at higher latitudes than the stations that provide the data to produce the index. The inability of the AL index to act as a sensitive indicator of substorm activity during weak activity such as discussed here has been documented before (see for example Baumjohann, 1986).

There was no evidence for a substorm growth phase prior to the second interval of Pi2 wave activity, the onset of which occurred at ~2118 UT during an interval of northward IMF, which had started at 2050 UT. If we take the time of the last Pi2 pulsation of the first interval of wave activity, 2049 UT, as the earliest time that the growth phase could have begun, the growth phase could only have lasted for 30 minutes. The minimum in the AL index was only −80 nT at ~2220 UT, some considerable time after the final Pi2 pulsation in interval 2. However, the contributing station to the AL index throughout the interval of substorm activity was Cape Chelyuskin which was located between 0400 and 0600 MLT, indicating that the location of the auroral break-up was probably poleward of all of the stations that contribute to AL.

The substorm expansion phase

To clarify the discussion here it is necessary to determine if one or two expansion phases occurred. Two intervals of Pi2 wave activity occurred, separated by about 30 minutes. There is, however, no strict definition of the time interval between substorm expansion phases. As mentioned above, there is no evidence for a second growth phase. Perhaps the best indicator that a separate expansion phase begun is the location of the auroral break-up, which cannot be determined here, but probably occurred to the east and poleward of the EISCAT field of view. The only evidence for auroral precipitation during the Pi2 wave activity was at EISCAT and only during the later stages of each interval. It is, therefore, perhaps prudent to conclude that the two intervals of wave activity actually represent one expansion phase.

The expansion phase onset of this second interval occurred at ~2019 UT. Although particle precipitation at EISCAT occurred on the scan starting at 2030 UT (~2300 MLT) and at latitudes above ~67°Λ there was no substorm associated signature in the EISCAT flow measurements. Likewise there was no associated signature in the Sondrestrom sector (1820 MLT) or Goose Bay sector (~1720 MLT).

Enhanced particle precipitation in the E region in the EISCAT local time sector (0000 MLT) occurred on the scan following the start of the second interval of wave activity, i.e. 2130 UT, and after the final intensification of this substorm. The response of the convection during this second period was somewhat variable. In the EISCAT sector, the main feature was increased eastward flow between 2130 and 2200 UT, which was related to the enhanced westward electrojet associated with the final intensification of this expansion phase. In the Sondrestrom sector, the main feature was the continued strong westward flow at latitudes ~70°Λ during an interval of northward IMF. The flow at higher latitudes remained predominantly equatorward during the expansion phase, consistent with flow out of the polar cap.

The possibility of an external trigger mechanism for the expansion phase onset at 2019 UT is unlikely. Up to 2040 UT the solar wind velocity and density remained fairly stable. The IMF was also stable, although there was a change of orientation at 2050 UT, from mainly directed in the negative X direction to the Y-Z plane with a positive Z component. This orientation was reversed at 2110, although the IMF remained slightly northward. Either of

these two reversals may have triggered the second interval of substorm activity at 2219 UT.

The recovery phase

Assuming that there was only a single expansion phase, the recovery phase began at 2143 UT, the time at which the X component at SOR reached its minimum value. This was after the final Pi2 pulsation in the expansion phase. The X component at SOR took about 2 hours to reach a value similar to that prior to the expansion phase. This implies an overall length for the substorm of over 4.5 hours, which would seem very long for a period of weak energy input from the solar wind as determined by the solar wind parameters.

6 Summary

Multi-point observations of ionospheric convection made during two intervals of variable IMF B_z and B_y which also contained a number of substorms have been described. The two intervals differed markedly and in summary we present a comparison of three features of the substorms during these intervals: the input conditions, the output level and the possible trigger mechanism. The input conditions are determined by the IMF and solar wind parameters. The solar wind energy input is normally regarded as being related to solar wind velocity, IMF magnitude and direction. The solar wind velocity during the two intervals was very similar; between 380 m s^{-1} and 420 m s^{-1} during interval 1 and between 420 m s^{-1} and 460 m s^{-1} in interval 2. On the other hand the IMF magnitude and orientation were very different. The magnitude was typically a factor of 2 higher in interval 1. The direction in interval 2 was primarily in the X direction, whereas in interval 1 there were significant components in all three directions.

The substorms themselves were also very different. It is difficult to compare absolute magnitudes of the energy released during each substorm because the stations were at different locations with respect to the auroral break ups. In interval 1, the expansion phase occurred at latitudes comparable to EISCAT and Sondrestrom but between the two. In interval 2, the expansion phase onset occurred poleward and to the east of EISCAT. The substorm in interval 1, however, could be regarded as the classical substorm: growth phase, in response to a southward turning of the IMF; expansion phase identified by Pi2 pulsations and auroral precipitation, with a number of intensifications; and a recovery phase during which the level of activity decreased and the electrojets and auroral precipitation contracted polewards. Most, if not all of the energy which had been transmitted from the solar wind into the magnetosphere had been released. Interval 2, however, was very different. The substorm activity comprised either of two separate substorm intervals or one single interval with an expansion phase which included a long interval, ~30 minutes between intensifications. The initial growth phase was long, as was the growth phase for the substorm in interval 1.

The trigger mechanism for the substorm expansion phases is unclear. The substorm in interval 1 may have been triggered by a northward turning of the IMF. However, in interval 2 the solar wind and IMF conditions are such that it is hard to identify any external triggering mechanism for the expansion phase. It is possible, however, that a change in the IMF orientation did result in the second interval of Pi2 wave activity. This may have been the reason why there was such a gap in the Pi2 wave activity.

One final point concerns the response of the ionospheric convection to the southward turning of the IMF. The ionospheric convection flow magnitude increased at all local times, but the response time varied with local time, increasing from ~20 minutes at ~1800 MLT to ~50 minutes near midnight. The overall length of the growth phase measured for the two substorms was 90 minutes, longer than that predicted by linear prediction filtering techniques (Bargatze *et al.*, 1985) or by a simulation of magnetosphere-ionosphere coupling (Kan *et al.*, 1988). In one case, there is evidence for a westward movement of the location of the evening flow reversal in response to the substorm. An example of a brief burst of equatorward flow during the growth phase of one substorm and apparently steady solar wind conditions was observed. Such variations in the ionospheric convection during the growth phase are of considerable interest at the moment.

Acknowledgements. We would like to thank Dr. E. C. Thomas for his efforts in maintaining the operation of the Wick radar. We would also like to thank the director and staff of the EISCAT radar for their efforts in keeping the radar operational during the extended run of Common Programmes. EISCAT is supported by the Suomen Akatemia (Finland), the Centre National de la Recherche Scientifique (France), the Max-Planck-Gesellschaft (Germany), the Norges Almenvitkenskapelige Forskingråd (Norway) the Naturveterskapliga Forskningsrådet (Sweden) and the Science and Engineering Research Council (United Kingdom). The Johns Hopkins University/Applied Physics Laboratory HF radar at Goose Bay, Labrador is supported in part by the National Science Foundation (NSF) Division of Atmospheric Sciences and the Air Force Office of Scientific Research, Directorate of Atmospheric and Chemical Sciences, under NSF grant ATM-8713982 and in part by the National Aeronautic and Space Administration (NASA) under the NASA grant 7055. Millstone Hill operations and analysis were supported by NSF grant ATM 88-08137 to the Massachusetts Institute of Technology. The Sondrestrom radar is supported by NSF grants ATM-8822560 and −9102439. We would like to thank Dr. R. P. Lepping for the provision of IMP-8 magnetometer data, Dr. A. Lazarus for the provision of IMP-8 plasma data, Dr. E. Friis-Christensen for the provision of magnetometer data from Greenland and the Geomagnetism Group, British Geological Survey for magnetometer data from Lerwick. ML would like to acknowledge the help of the CEDAR database.

References

Akasofu, S.-I., *Polar and Magnetospheric Substorms*, D. Reidel Publ. Co., 1968.

Akasofu, S.-I., The solar wind-magnetosphere coupling and magnetospheric disturbances, *Planet. Space Sci.*, **28**, 495, 1980.

Bame, S. J., A. J. Hundhausen, J. R. Asbridge and I. B. Strong, Solar wind ion composition, *Phys. Rev. Lett.*, **20**, 393, 1968.

Bargatze, L. F., D. N. Baker, R. L. McPherron and E. W. Hones, Jr., Magnetosphere Impulse Response for many Levels of Geomagnetic Activity, *J. Geophys. Res.*, **90**, 6387, 1985.

Baron, M., The EISCAT Facility, *J. Atmos. Terr. Phys.*, **46,** 469, 1984.

Baumjohann, W., Merits and limitations of the use of geomagnetic indices in solar wind-magnetosphere coupling studies, in *Solar Wind-Magnetosphere Coupling* (Eds. Y. Kamide and J. A. Slavin) Terra Sci. Pub. Co., 1986.

Baumjohann, W., The plasma sheet boundary layer and magnetospheric substorms, *J. Geomagn. Geoelectr.*, **40,** 157, 1988.

Beard, D. B., The Interaction of the Terrestrial Magnetic Field with the Solar Corpuscular Radiation, *J. Geophys. Res.*, **65,** 3559, 1960.

de la Beaujardière, O., R. Vondrak and M. Baron, Radar observations of electric fields and currents associated with auroral arcs, *J. Geophys. Res.*, **82,** 5051, 1977.

de la Beaujardière, O., V. B. Wickwar and J. H. King, Sondrestrom radar observations of the effect of the IMF B_y component on polar cap convection, in *Solar Wind-Magnetosphere Coupling* (Eds. Y. Kamide and J. A. Slavin) Terra Sci. Pub. Co., 1986.

de la Beaujardière, O., D. S. Evans, Y. Kamide and R. P. Lepping, Response of auroral oval precipitation and magnetospheric convection to changes in the interplanetary magnetic field, *Annal. Geophys.*, **5A,** 519, 1987.

Burrage, M. D., Radar studies of high latitude convection flows, Ph. D. Thesis, University of Leicester, 1988.

Caan, M. N., R. L. McPherron and C. T. Russell, Characteristics of the association between the interplanetary magnetic field and substorms, *J. Geophys. Res.*, **82,** 4837, 1977.

Clauer, C. R., J. D. Kelly, M. Lockwood, R. M. Robinson, J. M. Ruohoniemi, O. de la Beaujardière and L. Hakkinen, June 1987 GISMOS Experiment: Preliminary Report on High Time Resolution, Multi-Radar Measurements, *Adv. Space Res.*, **9(5),** 29, 1989.

Dudeney, J. R., A. S. Rodger, M. Pinnock, J. M. Ruohoniemi, K. B. Baker and R. A. Greenwald, Studies of Conjugate Plasma Convection in the Vicinity of the Harang Discontinuity, *J. Atmos. Terr. Phys.*, **53,** 249, 1991.

Dungey, J. W., Interplanetary magnetic field and the auroral zones, *Phys. Rev. Lett.*, **6,** 47, 1961.

Etemadi, A., S. W. H. Cowley, M. Lockwood, B. J. I. Bromage and D. M. Willis, The dependence of high-latitude dayside ionospheric flows on the north-south component of the IMF: A high time resolution correlation analysis using EISCAT "Polar" and AMPTE-UKS and IRM data, *Planet. Space Sci.*, **36,** 471, 1988.

van Eyken, A. P., H. Rishbeth, D. M. Willis and S. W. H. Cowley, Initial EISCAT observations of plasma convection at invariant latitudes 70°–77°, *J. Atmos. Terr. Phys.*, **46,** 635, 1984.

Foster, J. C., An empirical electric field model derived from Chatanika radar data, *J. Geophys. Res.*, **88,** 981, 1983.

Foster, J. C., D. H. Fairfield, K. W. Ogilvie and T. S. Rosenberg, Relationship of interplanetary parameters and occurrence of magnetospheric substorms, *J. Geophys. Res.*, **76,** 6971, 1971.

Foster, J. C., J. R. Doupnik and G. S. Stiles, Large scale patterns of auroral ionospheric convection observed with the Chatanika radar, *J. Geophys. Res.*, **86,** 11357, 1981.

Foster, J. C., J. M. Holt, R. G. Musgrove and D. S. Evans, Solar wind dependencies of high-latitude convection and precipitation, in *Solar Wind-Magnetosphere Coupling* (Eds. Y. Kamide and J. A. Slavin) Terra Sci. Pub. Co., 1986.

Freeman, M. P. and D. J. Southwood, The correlation of variations in the IMF with magnetosheath field variations, *Adv. Space Res.*, **8,** 217, 1988.

Freeman, M. P., C. J. Farrugia, S. W. H. Cowley, M. Lockwood and A. Etemadi, The response of the magnetosphere-ionosphere system to solar wind dynamic pressure variations, *Proc. Chapman Conf. Magnetic Flux Ropes,* pp 611, 1990.

Friis-Christensen, E., Y. Kamide, A. D. Richmond and S. Matsushita, Interplanetary magnetic field control of high-latitude electric fields and currents determined from Greenland magnetometer data, *J. Geophys. Res.*, **90,** 1325, 1985.

Goertz, C. K. and R. A. Smith, The thermal catastrophe model of substorms, *J. Geophys. Res.*, **94,** 6581, 1989.

Greenwald, R. A., K. B. Baker, R. A. Hutchins and C. Hanuise, An HF phased array radar for studying small-scale structure in the high-latitude ionosphere, *Radio Sci.*, **20,** 63, 1985.

Greenwald, R. A., K. B. Baker, J. M. Ruohoniemi, J. R. Dudeney, M. Pinnock, N. Mattin, M. Leonard and R. P. Lepping, Simultaneous conjugate observations of dynamic variations in high-latitude dayside convection due to changes in IMF B_y, *J. Geophys. Res.*, **95,** 8057, 1990.

Gussenhoven, M. S., D. A. Hardy and W. J. Burke, DMSP F2 Electron observations of equatorward auroral boundaries and their relationship to magnetospheric electric fields, *J. Geophys. Res.*, **86,** 768, 1981.

Heelis, R. A., The effects of interplanetary magnetic field orientation on dayside high-latitude ionospheric convection, *J. Geophys. Res.*, **89,** 2873, 1984.

Heppner, J. P. and N. C. Maynard, Empirical high-latitude electric field models, *J. Geophys. Res.*, **92,** 4467, 1987.

Hones, E. W., Jr., Transient Phenomena in the Magnetotail and their relation to substorms, *Space Sci. Rev.*, **23,** 393, 1979.

Kan, J. R., Developing a global model of magnetospheric substorms, *EOS (Trans. Am. Geophys. Union)*, **71,** 1083, 1990.

Kan, J. R., L. Zhu and S.-I. Akasofu, A theory of substorms: onset and subsidence, *J. Geophys. Res.*, **93,** 5624, 1988.

Kisabeth, J. L. and G. Rostoker, Current flow in auroral loops and surges inferred from ground-based magnetic observations, *J. Geophys. Res.*, **78,** 5573, 1973.

Lester, M., H. J. Singer, D. P. Smits and W. J. Hughes, Pi2 Pulsations and the substorm current wedge: low-latitude polarisation, *J. Geophys. Res.*, **94,** 17133, 1989.

Lester, M., M. P. Freeman, D. J. Southwood, J. A. Waldock and H. J. Singer, The expansion and contraction of the polar cap: A case study, *J. Geopyhs. Res.*, **95,** 21133, 1990.

Lockwood, M., The excitation of ionospheric convection, *J. Atmos. Terr. Phys.*, **53,** 177, 1991.

Lockwood, M. and S. W. H. Cowley, Observations at the magnetopause and in the auroral ionophere of momentum transfer from the solar wind, *Adv. Space Res.*, **8,** 281, 1988.

Lockwood, M., S. W. H. Cowley and M. P. Freeman, The excitation of plasma convection in the high-latitude ionosphere, *J. Geophys. Res.*, **95,** 7961, 1990.

Lühr H, S. Thürey and N. Klöcker, The EISCAT magnetometer cross. Operational Aspects – First Results, *Geophys. Surveys*, **6,** 305, 1984.

Lui, A. T. Y., A synthesis of magnetospheric substorm models, *J. Geophys. Res.*, **96,** 1849, 1991.

Lui, A. T. Y., A. Mankofsky, C.-L. Chang, K. Papadopoulos and C. S. Wu, A current disruption mechanism in the neutral sheet: A possible trigger for substorm expansion, *Geophys. Res. Lett.*, **17,** 745, 1990.

McPherron, R. L., Growth Phase of magnetospheric substorms, *J. Geophys. Res.*, **75,** 5592, 1970.

McPherron, R. L., Magnetospheric substorms, *Rev. Geophys. Space Phys.*, **17,** 657, 1979.

McPherron, R. L., C. T. Russell and M. P. Aubry, Satellite studies of magnetospheric substorms on August 15, 1968, 9. Phenomenological Model for Substorms, *J. Geopyhs. Res.*, **78,** 3131, 1973.

Moses, J. J., G. L. Siscoe, N. U. Crooker and D. J. Gorney, IMF B_y and day-night conductivity effects in the expanding polar cap convection model, *J. Geophys. Res.*, **92,** 1193, 1987.

Moses, J. J., G. L. Siscoe, R. A. Heelis and J. D. Winningham, Polar cap deflation during magnetospheric substorms, *J. Geophys. Res.*, **94,** 3785, 1989.

Nielsen, E., W. Guttler, E. C. Thomas, C. P. Stewart, T. B. Jones and A. Hedberg, A new radar auroral backscatter experiment, *Nature*, **304,** 712, 1983.

Pellinen R. J., W. Baumjohann, W. Heikkila, V. A. Sergeev, A. G. Yahnin, G. Marklund and A. O. Melnikov, Event study of pre-substorm phases and their relation to the energy coupling between solar wind and magnetosphere, *Planet. Space Sci.*, **30,** 371, 1982.

Reiff, P H. and J. L. Burch, IMF B_y-dependent plasma flow and Birkeland currents in the dayside magnetosphere: 2. A global model for northward and southward IMF, *J. Geophys. Res.*, **90,** 1595, 1985.

Rostoker, G. and T. G. Eastman, A boundary layer model for magnetospheric substorms, *J. Geophys. Res.*, **92,** 12187, 1987.

Rostoker, G. and J. V. Olson, Pi2 Micropulsations as indicators of substorm onsets and intensifications, in *Auroral Processes,* (Ed. C. T. Russell), Japan Scientific Societies Press, Tokyo, 1979.

Rostoker, G., S.-I. Akasofu, J. Foster, R. A. Greenwald, Y. Kamide, K. Kawasaki, A. T. Y. Lui, R. L. McPherron and C. T. Russell, Magnetospheric substorms – definition and signatures, *J. Geophys. Res.*, **85,** 1663, 1980.

Rostoker, G., S.-I. Akasofu, W. Baumjohann, Y. Kamide and R. L. McPherron, The roles of direct input of energy from the solar wind and unloading of stored magnetotail energy in driving magnetospheric substorms, *Space Sci. Rev.*, **46,** 93, 1987.

Rostoker, G. W. Baumjohann and C. T. Russell, A case study of the response of the magnetosphere to changes in the interplanetary medium, *J. Geophys. Res.*, **53,** 170, 1983.

Ruohoniemi, J. M., R. A. Greenwald, K. B. Baker, J.-P. Villain, C. Hanuise and J. Kelly, Mapping high-latitude plasma convection with coherent HF radars, *J. Geophys. Res.*, **94,** 13463, 1989.

Siscoe, G. L. and T. S. Huang, Polar cap inflation and deflation, *J. Geophys. Res.*, **90,** 543, 1985.

Smith, R. A., C. K. Goertz and W. Grossmann, Thermal catastrophe in the plasma sheet boundary layer, *Geophys. Res. Lett.*, **13,** 1380, 1986.

Spreiter, J. R. and S. S. Stahara, A new predictive model for determining solar wind-terrestrial planet interactions, *J. Geophys. Res.*, **85,** 6769, 1980.

Szuszczewicz, E. P., P. Wilkinson, W. Swider, S. Pulinets, M. A. Abdu, E. Roelof, T. Fuller-Rowell, T. Bateman, P. Blanchard, J. Foster, G. Gustafsson, R. Hanbaba, J. Joselyn, T. Kikuchi, R. Leitinger, M. Lester, B. Reddy, J. M. Ruohoniemi, M. Sands, J. Sobral, G. O. Walker and V. Wickwar, Measurements and empirical model comparisons of F-region characteristics and auroral oval boundaries during the solstitial SUNDIAL campaign of 1987, *Annal. Geopyhsicae.*, 1993.

Todd, H., S. W. H. Cowley, M. Lockwood, D. M. Willis and H. Lühr, Response time of the high latitude dayside ionosphere to sudden changes in the north-south component of the IMF, *Planet. Space, Sci.*, **36,** 1415, 1988.

Waldock, J. A., T. B. Jones and E. Nielsen, Mean auroral E-region plasma convection patterns measured by SABRE, *Nature*, **313,** 204, 1985.